IKP-MS-93/0302

Single Photon and Neutral Meson Production in Nuclear Collisions at 200 AGeV

WA80 Collaboration

INSTITUT FÜR KERNPHYSIK
UNIVERSITÄT MÜNSTER

Single Photon and Neutral Meson Production in Nuclear Collisions at 200 AGeV*

WA80 Collaboration

K.H. Kampert[4], R. Albrecht[1], T.C. Awes[5], F. Berger[4], M. Bloomer[2], D. Bock[4], G. Clewing[4], R. Debbe[6], L. Dragon[4], A. Eklund[3], R.L. Ferguson[5], S. Fokin[7], S. Garpman[3], R. Glasow[4], H.Å. Gustafsson[3], H.H. Gutbrod[1], O. Hansen[6], G. Hölker[4], J. Idh[3], M. Ippolitov[7], P. Jacobs[2], K. Karadjev[7], B.W. Kolb[1], A. Lebedev[7], H. Löhner[8], I. Lund[8], V. Manko[7], B. Moskowitz[6], F.E. Obenshain[5], A. Oskarsson[3], I. Otterlund[3], T. Peitzmann[4], F. Plasil[5], A.M. Poskanzer[2], M. Purschke[4], B. Roters[4], S. Saini[5], R. Santo[4], H.R. Schmidt[1], S.P. Sørensen[5,9], K. Steffens[4], P. Steinhaeuser[4], E. Stenlund[3], D. Stüken[4], A. Vinogradov[7], H. Wegner[6], and G.R. Young[5]

1. *Gesellschaft für Schwerionenforschung; D-6100 Darmstadt, Fed. Rep. of Germany*
2. *Lawrence Berkeley Laboratory, Berkeley, California 94720, USA*
3. *University of Lund, S-22362 Lund, Sweden*
4. *University of Münster, D-4400 Münster, Fed. Rep. of Germany*
5. *Oak Ridge National Laboratory, Oak Ridge, Tennessee 37831, USA*
6. *Brookhaven National Laboratory, Upton, New York 11973, USA*
7. *Kurchatov Institute of Atomic Energy, Moscow 123182, Russia*
8. *KVI, University of Groningen, NL-9747 AA Groningen, Netherlands*
9. *University of Tennessee, Knoxville, Tennessee 37996, USA*

Abstract

Employing a 3790 module lead-glass photon spectrometer the production of neutral pions, eta-mesons, and single photons has been studied in the interaction of 200 AGeV ^{32}S projectiles with a Au target. Transverse momentum spectra of π^0 have been measured for $0.3 \leq p_\perp \leq 4.0$ GeV/c and different classes of event centralities. The shape of the differential invariant cross section in peripheral S + Au collisions is similar to that of minimum-bias pA-interactions but a strong nuclear enhancement is observed at large values of $p_\perp$ in central S + Au reactions. The production of η mesons is found to be in agreement with $m_\perp$-scaling when compared to π^0 mesons. Very preliminary results on single photon to π^0 yields are presented and their experimental uncertainty is discussed.

1 Introduction

The primary motivation for studying high-energy heavy-ion collisions at the CERN-SPS and Brookhaven-AGS accelerators is to investigate nuclear matter under conditions of extremely high densities and temperatures. Theoretical calculations predict that under such conditions hadronic matter might undergo a phase-transition to a new form of matter, the quark-gluon plasma (QGP), in which quarks and gluons

*Invited talk presented at the "*2nd International Conference on Physics and Astrophysics of Quark-Gluon Plasma*", Calcutta, January 19 – 23, 1993 are deconfined over an extended volume [1]. Although the exact nature of such a phase-transition is still not without controversies, there is much interest in detecting appropriate signals of the expected new state of matter. A big obstacle in this effort is the complicated space-time evolution of the hot fireball, because the subsequent hadronization tends to mask the signal from the QGP phase. Among the various suggested signals thermal lepton pairs and direct photons share the advantage of acting as very clean probe of the plasma, because they interact only via the electromagnetic force and thus escape from the early high density stage without being disturbed by the later hadronization.

Direct photons have been measured at large transverse momenta ($p_\perp \gtrsim 3\,\mathrm{GeV}/c$) by various experiments using different beam particles ($\pi^\pm, p, \bar{p}$) and targets (p, nucleus) [2]. In these interactions their production arises from single hard processes and their yield can be calculated within the framework of pertubative QCD by employing experimentally measured hadronic structure functions [3, 4]. In case of a QGP, thermal direct photons are expected from the same kind of elementary processes, i.e. from quark-gluon Compton scattering ($qg \rightarrow q\gamma, \bar{q}g \rightarrow \bar{q}\gamma$) and quark-antiquark annihilation ($q\bar{q} \rightarrow g\gamma$). Their yield can be calculated in a similar way by integrating over the space-time history of the plasma phase [5, 6, 7, 8] and is expected to scale with the square of the number of charged particles and the cube number of the initial temperature of the system. This "black-body radiation" of the plasma is expected to dominate the region below $p_\perp \approx 3 - 4\,\mathrm{GeV/c}$. However, very recently it has been argued that also a hadron gas of sufficiently high temperature will radiate a substantial amount of photons [9] via processes of the kind $hh \rightarrow h\gamma$. The most abundant source of photons with sufficiently high energy is the $\pi\rho \rightarrow \pi\gamma$ reaction with an intermediate virtual π or ρ or $A_1(1260)$, with the latter one pointed out in Ref. [10]. The yield of such single photons together with those arising from $\pi\pi \rightarrow \rho\gamma$ and from radiative decays of higher resonances, e.g. $\omega \rightarrow \pi^0\gamma, \quad \eta \rightarrow \rho^0\gamma, \eta\gamma$ may dominate over the single photons from the plasma at $p_\perp \lesssim 1\,\mathrm{GeV/c}$, thus leaving an appropriate window for thermal photons from the plasma in the transverse momentum range $1.0 \lesssim p_\perp \lesssim 4\,\mathrm{GeV/c}$ [11]. The standard sources of single photon production and the ingredients of theoretical calculations are sketched in Table 1.

The WA80 collaboration has concentrated on the measurement of single photons by a large acceptance lead-glass array. Since most of the observed photons arise from the $\pi^0 \rightarrow \gamma\gamma$ and $\eta \rightarrow \gamma\gamma$ decay, a careful investigation of these photon sources is required. The measurement of high precision transverse momentum distributions of produced particles, however, is interesting in its own right as ever since the discovery of hard scattering processes at the CERN ISR [12] $p_\perp$ spectra have been proven a valuable tool in the study of the properties of the compressed and highly excited reaction zone. To distinguish different contributing processes to particle production and to provide a reliable basis for comparisons with $p + p$ or $p + A$

scattering, a large $p_\perp$ coverage is required. In particular, data at high $p_\perp$ values, where hard or semi-hard processes become important and may be calculated by pertubative QCD, are of great interest. Also, there is still an unsettled discussion on the existence of a low-$p_\perp$ enhancement in nuclear reactions [13]. The present investigation of identified π^0's has therefore concentrated on the transverse momentum range $0.3 \leq p_\perp \leq 4.0$ GeV/c and on selections of the data according to the centrality of the reaction. Previous results on a related analysis based on O + Au data at 200 GeV/c have been reported in Refs. [14, 15].

2 Experimental Setup and Data Reduction

The experiment has been performed at the CERN SPS using the WA80 setup as shown in Fig. 2. Compared to the previous runs with ^{16}O ions, the distance of the photon detector to the target has been increased to 9 m. Furthermore, the Saphir detector which comprises 1278 lead-glass modules [16] has been extended by two towers with 1256 modules each. In the present setup the experimental coverage subtends $2.1 \leq \eta \leq 2.9$. Two layers of Iarrocci-type streamer tube detectors with pad readout [17] are used as charged particle veto-detector to reduce the background of charged hadrons in the photon sample. The combined efficiency of both planes is close to 98 %. The trigger and event selection is obtained by means of a uranium

Single Photons from A-A Collisions			
	Hadron Gas	***QGP***	***NN-Collisions***
Elementary processes:	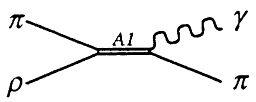 $\pi\pi \to \rho\gamma$ $\omega \to \pi^0\gamma$ $\eta \to \rho^0\gamma$, $\eta\gamma$... ⋮	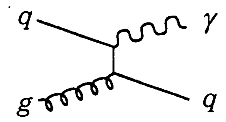 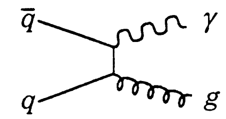	QCD - Compton QCD - Annihilation
Distribution:	Thermal (ε, T, S_{HG},...) + radiative decays	Thermal (ε, T, S_{QGP},...)	Structure Functions (experiment)
Total Yield:	Integration over Space-Time History		Superposition of *NN*-Collisions
Relevant Range:	Resonance Decays $p_\perp \leq 2$ GeV/c	"Thermal" Photons $p_\perp \approx 1$–4 GeV/c	"Direct" Photons $p_\perp \geq 4$ GeV/c

Table 1: Sources of single photon production in AA collisions.

scintillator sampling calorimeter located at zero degree [18], accompanied by an iron scintillator calorimeter located at mid-rapidity [19].

The data processing and in particular the reconstruction of π^0 and η mesons by invariant mass analysis has been described in detail in Ref. [16]. A new and fast photon and hadron identification method based on the lateral profile of the observed showers in the calorimeter has been developed over the past two years. Particular attention is paid to the additional complications arising from the operation of the detector in the high particle density environment of high energy nuclear collisions. To identify overlapping showers and to separate photons from accompanied close by hadrons or other photons, a shower unfolding procedure had to be developed and was proven to work well down to relative shower distances as close as 1.5 module units. Details of this procedure and its performance for applications in high energy heavy-ion reactions are described in Ref. [20].

Among the most important experimental difficulties in measuring single photons in high energy nuclear collisions is the precise determination of the photon and π^0 reconstruction efficiency, ε_γ and ε_{π^0}, respectively. The calculation is based on the actual experimental data and is performed by superimposing single hadronic and electromagnetic showers on a raw-data level to the measured heavy-ion events. The additional showers are either generated by the GEANT simulation package and assuming phase space distributions of the various particles according to the exper-

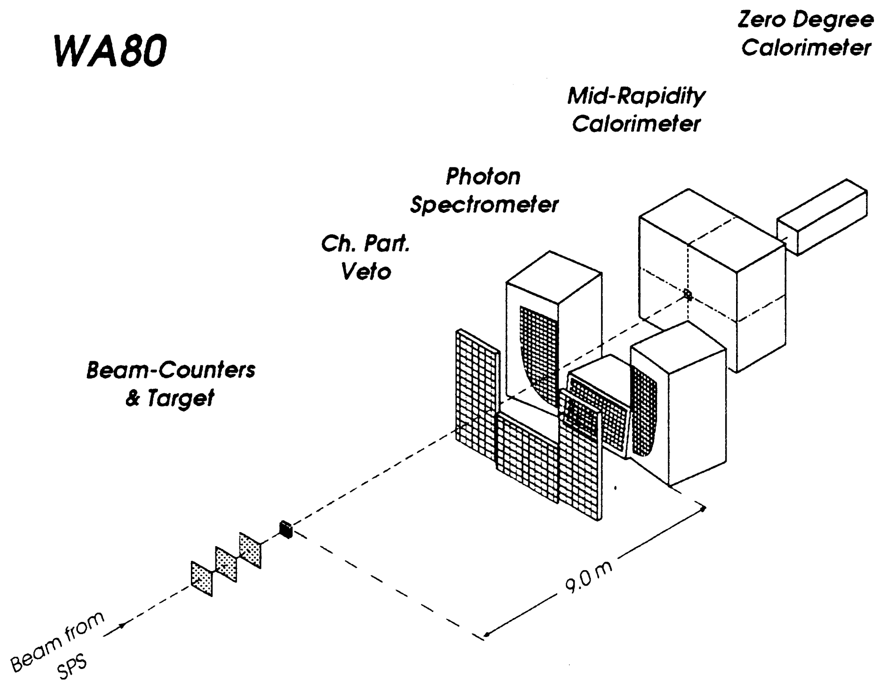

Fig. 1: Schematic view of the WA80 setup as of 1990/91.

imental data or are, for reasons of consistency checks, taken from very peripheral S + Au reactions. The artificial events are processed with the same chain of shower reconstruction routines as is used for real data events. The photon reconstruction efficiency is then defined by the ratio of the reconstructed photon spectrum divided by the known input photon spectrum and is found to depend both on the local particle density and on the transverse momentum of the photon. As a typical result for central S + Au events, an event-by-event correction according to $\varepsilon_\gamma(\varrho_{\mathrm{local}}, p_\perp,)$ leads to a change of the inverse slope parameter in the inclusive photon $p_\perp$-distributions from $T_{\mathrm{raw}} = 210\,\mathrm{MeV}$ to $T_{\mathrm{corr}} = 207\,\mathrm{MeV}$. The systematic and statistical uncertainty in the photon (and π^0) reconstruction efficiency is found to be approximately 3 %.

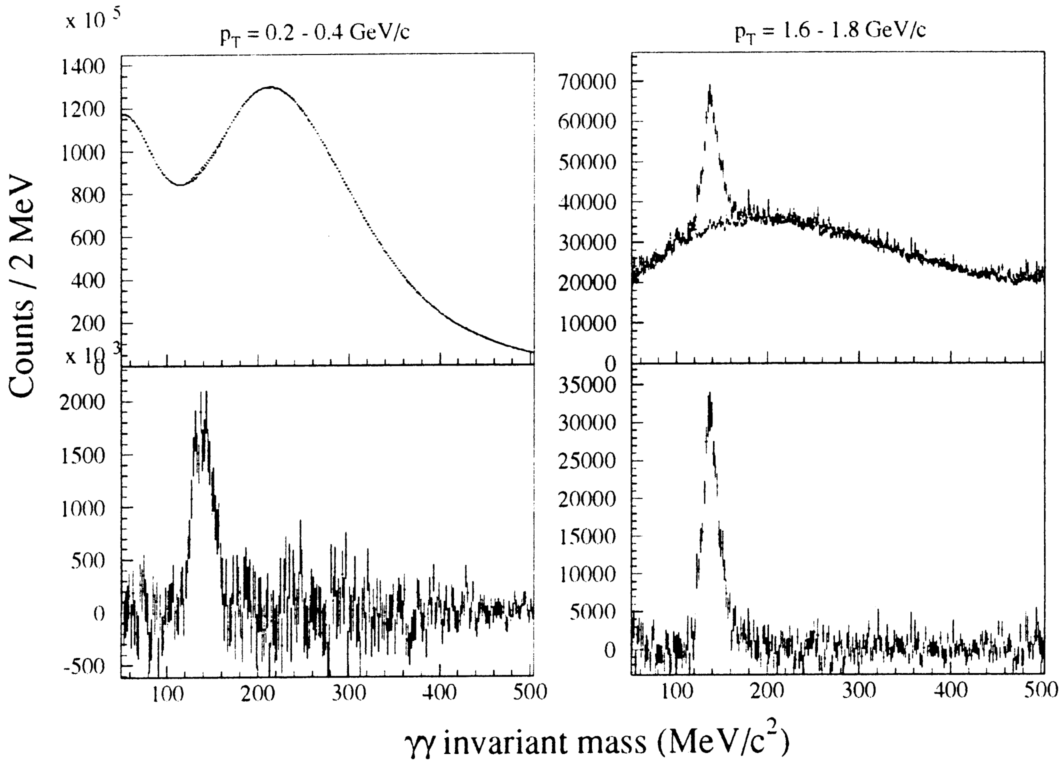

Fig. 2: Two photon invariant mass distributions for 200 AGeV S + Au collisions. The photon pairs are selected according to their transverse momentum (left panel: $0.2 \leq p_\perp \leq 0.4\,\mathrm{GeV/c}$, right panel: $1.6 \leq p_\perp \leq 1.8\,\mathrm{GeV/c}$). The two upper graphs represent the original invariant mass distributions and the lower graphs show the same data after subtraction of the combinatorial background generated from mixed events.

Differential cross sections of π^0 and η mesons are obtained by measuring their yields above the combinatorial background in invariant mass distributions of $\gamma\gamma$ pairs selected according to the variable of interest. A typical example is shown in Fig. 2 (top), where the $\gamma\gamma$ invariant mass distributions from 200 AGeV S + Au reactions are displayed for different $p_\perp$ bins. While there is no particular difficulty in extracting a π^0 signal in the high $p_\perp$ bin, the problem of observing a clear peak and extracting the corresponding π^0 yield above the background is immediately realized for the low $p_\perp$ bin, i.e. in the region of very large phase space density. However, a very powerful tool to determine the precise shape (and yield) of the background under the $\pi^0(\eta)$ peak is provided by the mixed event method. Here, the invariant mass distribution is constructed by combining photons from one event with those from another one of the same global characteristics. The result of such an analysis is shown in the lower part of Fig. 2 where the difference of the real data and mixed-event distribution is plotted. The clear structure of the π^0 decay is now easily identified even down to peak/total ratios as low as 0.15 %. In fact, the detectability in case of non-vanishing geometrical acceptance is in practice only limited by the statistics of the data sample. In the present data, π^0's could be identified down to $p_\perp = 0.1\,\mathrm{GeV/c}$ and η mesons down to $p_\perp \simeq 0.5\,\mathrm{GeV/c}$. In case of π^0's there are, however, at present still rather large systematic uncertainties in this region because of the poor geometrical acceptance and the influence of the low-energy threshold of the detector.

3 Results

3.1 π^0 *Transverse Momentum Spectra*

Preliminary invariant π^0 cross sections for minimum bias, central, and peripheral S + Au reactions are shown in Fig. 3 as a function of $p_\perp$. Compared to the previous O + Au data [14], the new data extend the $p_\perp$ range appreciably and cover now momenta up 4 GeV/c, allowing a first exploration of the hard scattering domain. Comparing the shapes of the two distributions in Fig. 3 (left) a remarkable flattening of the spectra with increasing centrality is observed. This can be verified more quantitatively by performing simple exponential fits to the data in the transverse momentum range $0.5 \leq p_\perp \leq 2.0\,\mathrm{GeV/c}$. The extracted inverse slope parameter increases from $T = 198\,\mathrm{MeV/c}$ in peripheral to $T = 225\,\mathrm{MeV/c}$ in central collisions. However, the deviation observed between the concave shaped experimental distributions and the extrapolated pure exponential function demonstrates that there is more information contained in the transverse momentum spectra than just the inverse slope parameter, T, extracted from a limited $p_\perp$ region. The excess of the experimental differential cross section over an exponential distribution is commonly referred to as the "low and high $p_\perp$ enhancement". The high $p_\perp$ enhancement has become a well known experimental fact which was first established in high energy pp [12] and pA reactions [21] where it has been ascribed to hard scattering phenomena [22] and multiple low-momentum scattering of partons inside the nuclear matter [23], respectively. There is, however, still experimental controversy about the occurrence of a low $p_\perp$ enhancement, first observed in high energy heavy ion

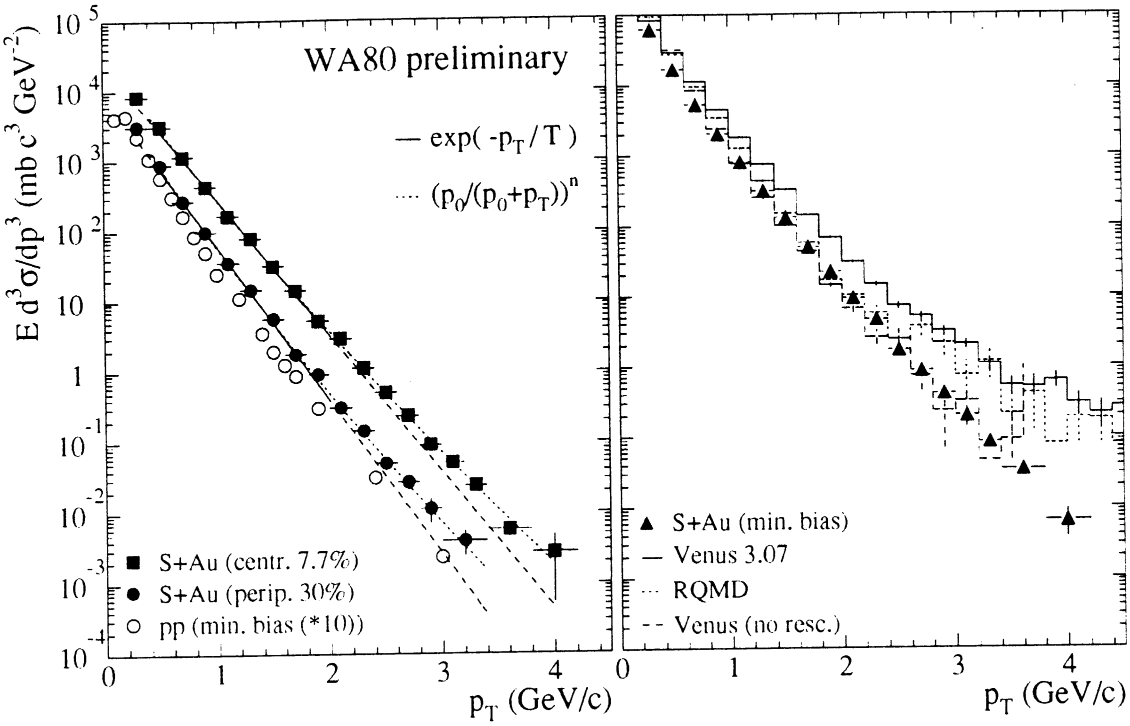

Fig. 3: Transverse momentum distributions of π^0 measured in $2.1 \leq \eta \leq 2.9$ for minimum bias (right), peripheral, and central (left) 200 AGeV S + Au reactions. The numbers in brackets give the percentage of the minimum bias cross section. The solid lines represent results of exponential fits to the data in the range $0.5 \leq p_\perp \leq 2.0$ GeV/c with the the inverse slope parameters $T_{centr} = 225$ MeV/c and $T_{peri} = 198$ MeV/c . The dashed line is the extrapolation of the exponential to lower and larger values in $p_\perp$. The dotted curves represent fits according to Eq. 1 with the parameters given in Table 2. Results of minimum bias pp collisions [12] are shown for comparison. The right panel shows a comparison of the data to different model predictions.

reactions (Recent reviews on this topic can be found in Refs. [13, 24, 25]). We would like to remark that, due to the above given definition by an arbitrarily chosen fit region of the exponential, there is some arbitrariness not only in the quoted slope parameters, but also in the quoted strength and in the regions of the low and high $p_\perp$ enhancement. This should be kept in mind when comparing such numbers from different experiments. Furthermore, the reliability and precision of of such a method suffers from the large extrapolation of an exponential distribution over many orders of magnitude in cross section by applying fit parameters which are defined by only very few data points.

As an alternative and more robust approach we have instead analyzed the the variation of the inverse local slope parameter as a function of $p_\perp$. Results of such an analysis are presented in Fig. 4. In general, a strong increase of the local slope by approximately 50 % is observed with increasing $p_\perp$, both for S + Au and and for p + p collisions. The largest difference is found between the central and peripheral S + Au data where significantly higher slope parameters are measured in the low and intermediate transverse momentum range of central collisions. At $p_\perp \simeq 3$ GeV/c both data sets approach the largest slope parameter of approximately $T_{\rm local} \approx 260$ MeV/c. The values of the p + p data closely resemble the peripheral S + Au data, but are in general slightly lower. *

The results from the numerical analysis of the local slopes are independently confirmed by fitting an empirical QCD inspired expression [26]

$$E\frac{d^3\sigma}{dp^3} = C \cdot \left(\frac{p_0}{p_0 + p_\perp}\right)^n \qquad (1)$$

to the entire $p_\perp$ distribution ($p_\perp \geq 0.5$ GeV/c). This provides an excellent fit over the *full range* of experimental data with the free parameters C, p_0, and n. Results of such a fit are included as dotted lines in Fig. 3 (left) and the fit parameters are compiled in Table 2, again in comparison with the results from p + p and p + A data. Since the fits describe all experimental data points well within their error bars and without systematic deviations, the local slope can be calculated from the derivative of Eq. 1, yielding

$$T_{\rm loc} = \frac{p_0 + p_\perp}{n} . \qquad (2)$$

The ratio p_0/n thus reflects the slope extrapolated to $p_\perp = 0$, and $1/n$ describes the gradient of the spectral slope per unit bin in $p_\perp$. Such an analysis (see Tab. 2) yields within the experimental error bars the same results as discussed above (Fig. 4). The smooth variation of the parameters when going from p + p to p + A, and further to peripheral and central S + Au reactions suggests an increasing flattening of the transverse momentum spectra particularly in the low and intermediate $p_\perp$ region ($\approx 0.5 - 2$ GeV/c) and a decreasing gradient of the slope parameter, i.e. the weakest curvature of the spectra in central heavy-ion reactions.

The importance of measuring spectra of identified particles up to large values of $p_\perp$ is obvious also from a comparison of the data to different model predictions, as shown in Fig. 3 (right). Disregarding some uncertainties of the absolute cross sections, which might be due to trigger effects, all three model predictions (VENUS with and without rescattering [27], and RQMD [28]) agree with the shape of the experimental distributions up to $p_\perp \approx 2$ GeV/c. However, large deviations both to the data and among the models themselves are observed at $p_\perp \approx 4$ GeV/c. Here,

*In order to allow for such a comparison, the p + p data were corrected for their slightly higher center of mass energy ($\sqrt{s} = 23$ GeV compared to $\sqrt{s} = 19.7$ GeV in S + Au) by applying an empirical scaling law extracted from ISR data [12, 13].

Table 2: Parameters obtained from fitting Eq. 1 to experimental data.

System	p_0/n (MeV/c)	$1/n$ ($\times 10^3$)	χ^2/NDF
200 GeV p + p [12]	134±3	35.7±1.2	47.8/36
200 GeV p + Au [14]	164±16	27.7±15.5	30.9/13
200 GeV S + Au (peri.)	170±6	26.5±4.7	17.6/10
200 GeV S + Au (centr.)	200±5	20.9±2.9	31.0/13
200 GeV O + Au (centr.)	187±11	22.2±6.8	20.1/22

VENUS without rescattering underestimates the experimental cross section while RQMD and in particular VENUS with rescattering predicts a too large cross section by more than one order of magnitude.

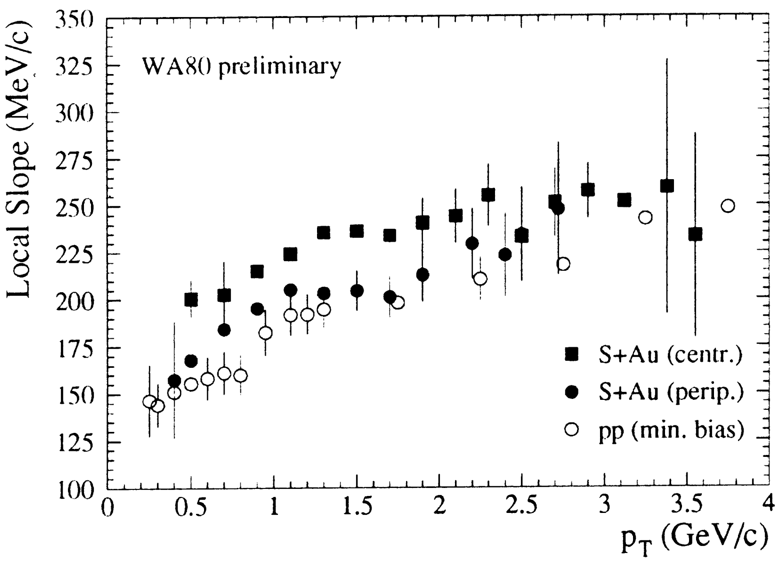

Fig. 4 Variation of local slopes $T_{\rm loc}$ as obtained numerically from adjacent data points.

The transverse momentum distributions of different systems can in a model independent way also be compared by calculating the ratios of spectra. Such a representation of data has previously been chosen by Cronin *et al.* [21] to discuss the nuclear enhancement of p + A over p + p reactions. A similar enhancement is now observed within the same system, but selecting different regions of impact parameters as is shown for S + Au data in Fig. 5. In accordance to the findings from the local slope parameters, the π^0 production from central S + Au reactions exhibits a relative enhancement over peripheral S + Au reactions by about a factor of 4 at large values of $p_\perp$.

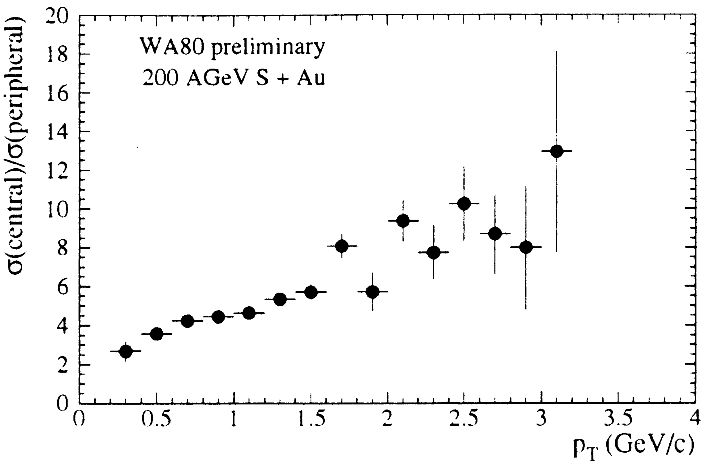

Fig. 5: Ratio of the π^0 $p_\perp$ spectra from central and peripheral S + Au reactions at 200 AGeV.

3.2 η Meson Production

The yield and spectral shape of η mesons is an important ingredient in the calculation of the direct photon production (see below), and is also an interesting quantity in its own. The quark composition of the η is given by $|\eta\rangle = \alpha(|u\bar{u}\rangle + |d\bar{d}\rangle) - \beta|s\bar{s}\rangle$ with $\beta \approx 0.9$, i.e. the η meson is a carrier of hidden strangeness and its relative abundance over π^0 mesons provides important information about the chemical composition of the compressed and hot matter. Their production has been studied with the same apparatus by measuring the $\eta \rightarrow \gamma\gamma$ decay. Because of the 2γ branching ratio of 38.9 % and the approximately 4-times larger opening angle of the decay photons, the acceptance is considerably reduced as compared to π^0 mesons. Using the mixed event method described above, an identification could be achieved in $0.5 \lesssim p_\perp \lesssim 2.5$ GeV/c with a typical invariant mass spectrum shown in Fig. 6. The peak position and its width are well within the expected values.

A preliminary η/π^0 ratio is presented in Fig. 7 as a function of $p_\perp$ with a typical invariant mass distribution shown in Fig. 6. The ratio is found to increase with $p_\perp$ in accordance with expectations from $m_\perp$-scaling. The result of a $m_\perp$-scaling fit performed to the heavy-ion data points is shown as hatched area. The extrapolated results are well in agreement with the η/π^0 ratio extracted from p + C reactions at the same energy and large values of $p_\perp$ [29] and are of similar experimental uncertainty.

3.3 Single Photon Production

The direct photon yield – commonly expressed in terms of the γ/π^0-ratio – is extracted from the measured photon yield N_γ and π^0 yield N_{π^0} according to the expression [2, 15]:

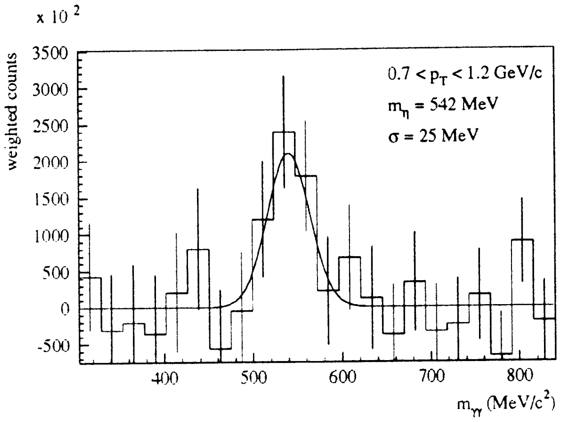

Fig. 6: Two-photon invariant mass spectrum from 200 AGeV S + Au reactions after background subtraction showing the η-meson peak.

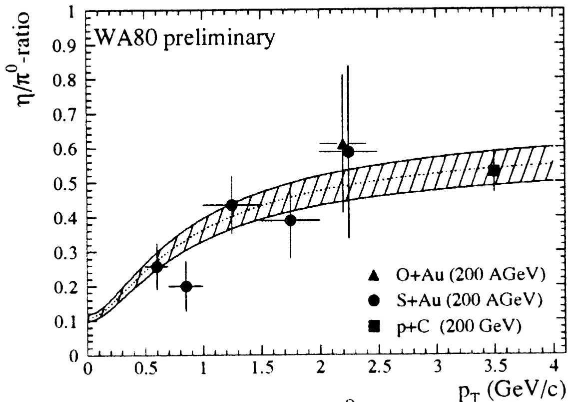

Fig. 7: Extracted η/π^0 ratio as a function of $p_\perp$ from O+Au and S+Au reactions together with results from p+C interactions at 200 GeV [29] and a fit to the heavy-ion data assuming $m_\perp$-scaling.

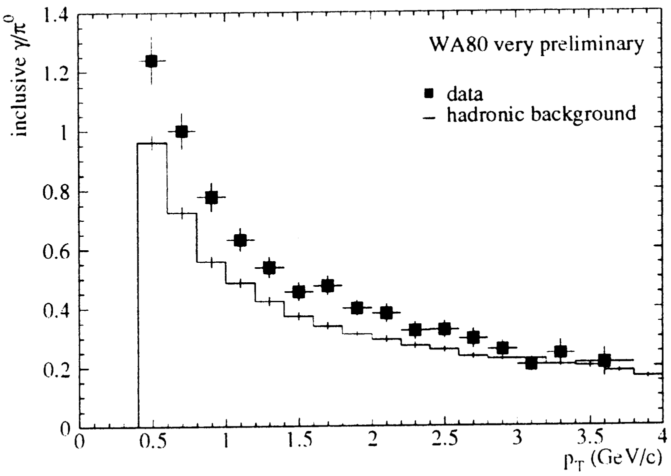

Fig. 8: Preliminary ratio of the inclusive γ/π^0 cross section as function of $p_\perp$ for minimum bias 200 AGeV S+Au reactions.

$$\frac{\gamma}{\pi^0} = \frac{N_\gamma}{N_{\pi^0}} \cdot \frac{\varepsilon_{\pi^0}}{\varepsilon_\gamma} \cdot A_{\rm geo} - (R_{\pi^0} + R_\eta + R_X) \qquad (3)$$

where ε_{π^0} and ε_γ are the photon and π^0 reconstruction efficiencies, respectively, $A_{\rm geo}$ is the geometrical acceptance of the detector for π^0's, and R_{π^0}, R_η, and R_X are the Monte-Carlo calculated ratios of observed background photons from measured π^0 and η mesons, and higher (non-measured) resonances, respectively. Such a presentation of data has the advantage that certain experimental errors, e.g. the absolute cross section normalization, cancel out thus allowing a total experimental sensitive in the γ/π^0 ratio of up to 5 %.

In case of high heavy-ion reactions where the π^0 and η production cross sections are in principle unknown it is very important to measure those data in the same experiment and in the appropriate $p_\perp$ region. Heavier resonances are then to a large part automatically taken already into account, since the major fraction of these resonances decays via the π^0 or η branch (e.g. $\eta' \to \pi^0\pi^0\eta$) and is therefore already contained in the measured spectra. Besides the π^0 decay the most important hadronic photon background is the $\eta \to \gamma\gamma$ decay. These photons amount to approximately 10 % compared to those from the π^0 while the sum of all heavier resonances contributes on the 1–2 % level. Possible inherent systematic uncertainties when assuming their production cross-sections from different experiments and reactions are thus suppressed by approximately the same factor.

In Fig. 8 we compare the total yield of background photons, as calculated by the Monte-Carlo, to the measured inclusive photon yield as a function of $p_\perp$. In this very preliminary ratio an excess of photons over the background calculation is observed at low $p_\perp$. However, further analysis is still required to estimate the influence of photon conversion and other remaining effects, like nonlinearities, etc., in order to verify this interesting experimental finding.

4 Summary

Impact parameter selected transverse momentum distributions of π^0 have been measured for 200 AGeV S + Au reactions in the pseudorapidity range $2.1 \leq \eta \leq 2.9$. The spectral shape of the invariant π^0 cross sections is analyzed (*i*) by extracting the local slope from the spectra, (*ii*) by fitting a formula proposed by Hagedorn, and (*iii*) by calculating ratios of spectra. All these results clearly demonstrate that simple exponential fits are inappropriate to describe the concave shaped experimental distributions. At $p_\perp \simeq 3$ GeV/c a slope parameter of $T_{\mathrm{loc}} \simeq 260$ MeV/c is observed for all systems. In the intermediate transverse momentum range ($0.5 \lesssim p_\perp \lesssim 2.0$ GeV/c) we observe a gradual increase of the inverse slope parameter when going from minimum bias p + p via minimum bias p + A and peripheral S + Au to central S + Au reactions.

String models like VENUS or RQMD provide a rather good description of the data in the low and intermediate $p_\perp$ range but totally fail in describing the spectra at $p_\perp \gtrsim 3$ GeV/c.

The production of η-mesons is in agreement to expectations from $m_\perp$-scaling when compared to π^0's. The preliminary η/π^0 ratio extracted from S + Au reactions and extrapolated to large values of $p_\perp$ is $\eta/\pi^0 = 0.56 \pm 0.07$ and is similar to results from p + C reactions.

A first and very preliminary estimate of the single photon yield is presented for 200 AGeV S + Au reactions. Subtracting all known sources of photons, most abundantly the decay photons from π^0 and η mesons a slight excess over the hadronic background is observed. Single photons from a hadron gas during the mixed phase would be a natural source of such photons. However, further detailed analyses is still required and presently underway to reduce the uncertainty in the γ/π^0 ratio to approximately 7 % at intermediate $p_\perp$, enabling us to set constrains on the initial and critical temperature of the interacting system.

Acknowledgment
It is a pleasure to warmly thank the organizers for their invitation and for setting up this interesting and successful conference on Quark-Gluon Plasma physics and. Partial support by the West German BMFT, GSI, the Indo-German fond, the United States DOE, the Swedish NFR, and the CERN PPE Division is gratefully acknowledged. In preparing this talk I have significantly profited from active support by my colleagues G. Hölker and G. Clewing who have carried out a large part of the data analysis presented in this proceedings.

References

[1] See most recent Quark Matter proceedings; *Nucl. Phys.* **A544** (1992), *Nucl. Phys.* **A525** (1991), *Nucl. Phys.* **A498** (1989), *Z. Phys.* **C38** (1988).
[2] T. Ferbel and W.R. Molzon, *Rev. Mod. Phys.* **56** (1984) 181.
[3] J.F. Owens, *Rev. Mod. Phys.* **59** (1987) 465–503.
[4] P. Aurenche et al., *Nucl. Phys.* **B297** (1988) 661–696.
[5] F. Halzen and H.C. Liu, *Phys. Rev.* **D25** (1982) 1842.
[6] R.C. Hwa and K. Kajantie, *Phys. Rev.* **D32** (1985) 1109.
[7] L.D. McLerran and T. Toimela, *Phys. Rev.* **D31** (1985) 545.
[8] B. Sinha, *Nucl. Phys.* **A459** (1986) 717–731.
[9] J. Kapusta, P. Lichard, and D. Seibert, *Phys. Rev.* **D44** (1991) 2774–2788.
[10] L. Xiong, E. Shuryak, and G.E. Brown, *Phys. Rev.* **D46** (1992) 3798–3801.
[11] S. Chakrabarty et al., *Phys. Rev.* **D46** (1992) 3802–3806.
[12] B. Alper et al., *Nucl. Phys.* **B100** (1975) 237–290.
[13] J. Schukraft, In V. Bernard et. al., editor, *Quark Gluon Plasma Signatures*, 127–143, Edition Frontiers, (1991).
[14] R. Albrecht et al., WA80-Collaboration, *Z. Phys.* **C47** (1990) 367–375.
[15] R. Albrecht et al., WA80-Collaboration, *Z. Phys.* **C51** (1991) 1–10.
[16] H. Baumeister et al. *Nucl. Instr. Meth.* **A292** (1990) 81–96.
[17] R. Albrecht et al., *Nucl. Instr. Meth.* **A276** (1989) 131.
[18] G.R. Young, et al., *Nucl. Instr. Meth.* **A279** (1989) 503–517.
[19] T.C. Awes, et al., *Nucl. Instr. Meth.* **A279** (1989) 479–502.
[20] F. Berger et al., *Nucl. Instr. Meth.* **A321** (1992) 152–164.
[21] J.W. Cronin and et al., *Phys. Rev.* **D11** (1975) 3105.
[22] M. A. Faessler, *Phys. Rep.* **115** (1984) 1–91.
[23] M. Lev and B. Petersson, *Z. Phys.* **C21** (1983) 155.
[24] H.R. Schmidt and J. Schukraft, Preprint: GSI-92-19 (1992).
[25] J. Stachel and G.R. Young, *Ann. Rev. Nucl. Part. Sci.* **42** (1992) 537–597.
[26] R. Hagedorn, CERN-TH 3684, (1983).
[27] K. Werner, proceedings to this conference.
[28] H. Sorge, H. Stöcker, and W. Greiner, *Nucl. Phys.* **A498** (1989) 567c–576c.
[29] J. Povlis, J. Biel, C. Bromberg, and et al., *Phys. Rev. Lett.* **51** (1983) 967.